Ohse *et al. Journal of Wood Science* (2022) 68:19
https://doi.org/10.1186/s10086-022-02027-4

Journal of Wood Science

ORIGINAL ARTICLE Open Access

Sequent periderm formation and changes in the cellular contents of phloem parenchyma during rhytidome development in *Cryptomeria japonica*

Megumi Ohse[1], Rika Irohara[1], Etsushi Iizuka[1], Izumi Arakawa[1,2], Peter Kitin[2,3], Ryo Funada[1,2] and Satoshi Nakaba[1,2*]

Abstract

The outer bark that includes sequent periderms is referred to as rhytidome. The defense and physiological functions of rhytidome are maintained by the continuous formation of sequent periderms. To understand the mechanisms of rhytidome growth, we examined the development of sequent periderms and the corresponding changes in the cellular contents of phloem parenchyma cells in *Cryptomeria japonica*. New layers of rhytidome were formed in the studied trees during the two-year course of the study. Our records showed that a new layer of periderm forms annually, and therefore, rhytidome development in *C. japonica* can be studied by sequential sample collection in any given year. Formation of new periderm and initiation of nuclei disappearance in phloem parenchyma in the outer layers of the developing outer bark occurred simultaneously. The early disappearance of nuclei indicates that some parenchyma cells might have been in a stage of preparation for cell death before the formation of new periderm. Four developmental stages of annual rhytidome growth were identified by structural and physiological changes of the outer layers of phloem parenchyma and the growth of the new periderm.

Keywords: Bark, *Cryptomeria japonica*, Phellogen, Rhytidome formation, Secondary phloem

Introduction

Bark includes all tissues outside the vascular cambium [1–3]. Bark tissues can be divided into inner bark and outer bark. The inner bark, which consists of secondary phloem, plays important roles in transportation and storage of photosynthetic products. In contrast, the outer bark, which consists of periderms and the tissues isolated by them, functions to protect from abiotic and biotic stresses. The periderm is a secondary protective tissue that is produced by phellogen (cork cambium) and contains phellem (cork), phellogen, and phelloderm. The innermost periderm is part of the outer bark and constitutes the boundary between the inner and outer bark [3]. The outer bark that includes sequent periderms is referred to as rhytidome [3]. In species that form rhytidome, sequent periderms arise at varying intervals of time in successively deeper layers of bark [4]. During rhytidome formation, color changes of cell walls and cell death of parenchyma cells occur in the secondary phloem, which is isolated between the new periderm and the previous periderm. Because older layers of rhytidome can gradually fall off the tree, the defense and physiological functions of the outer bark are maintained by formation of new rhytidome layers. Therefore, elucidation of the mechanism of sequent periderm formation and the corresponding physiological and morphological changes of the phloem cells located between the new and previous

*Correspondence: nakaba@cc.tuat.ac.jp
[1] Faculty of Agriculture, Tokyo University of Agriculture and Technology, 3-5-8 Saiwai-cho, Fuchu, Tokyo 183-8509, Japan
Full list of author information is available at the end of the article

periderms is important for understanding the details of bark physiology and the defense mechanisms of trees.

The first periderm and sequent periderms differ with regard to the origin of the phellogen and the timing of their appearance [2]. The epidermis, the first protective layer in plants, is strained tangentially by radial growth, eventually leading to its collapse. Prior to the destruction of the epidermis, phellogen is formed from epidermal or cortical parenchyma cells, and produces the first periderm to protect the inner living tissue [2, 4]. The first periderm that replaces the epidermis is formed in the first year of stem and root growth [2, 4]. In contrast, sequent periderms may be initiated later the same year as or many years after the formation of the first periderm or may never appear [2]. Sequent periderms originate in deeper tissue than the first periderm, usually in nonconducting phloem [3]. In addition, Mullick and Jensen [5] and Mullick [6] proposed that periderms could be classified into two categories, namely necrophylactic and exophylactic, depending on the site of periderm formation and the coloration of phellem cells. Thus, as mentioned above, periderms have been categorized according to their origin, timing of appearance, and site of formation.

Research on periderm formation has been performed, for the most part, with the first periderm. Previous studies have identified factors that might affect the formation of the first periderm, such as light intensity [7, 8], photoperiod [9, 10], temperature [9, 11], position of leaves and buds [8, 12] and plant hormones [8, 9]. In contrast, limited information is available on the mechanism of sequent periderm formation. Mullick [6] suggested that sequent periderm formation might be induced whenever the previous phellogen becomes non-functional. However, the cellular and molecular mechanisms of sequent periderm formation remain to be clarified.

In terms of periderm development during rhytidome formation, the characteristics and formation of phellem have been widely studied due to its economic importance in cork products [13]. The cell wall microstructure and chemical composition of phellem and its cellular and molecular mechanisms of formation have been reported in various tree species such as *Betula, Populus* and *Quercus* [14–20]. However, information about other phenomena during rhytidome formation such as changes in cellular contents in secondary phloem tissue that is isolated by periderms, and the seasonal development of sequent periderms, remains limited.

The main goal of the present study was to investigate the histological process of rhytidome formation in *Cryptomeria japonica*. *Cryptomeria japonica* is the dominant tree species for plantation in Japan, and has relatively simple xylem and phloem structure [21]. Therefore, *C. japonica* has been effectively used as a model in ecophysiological studies [22–25]. We studied the formation of sequent periderms leading to rhytidome development. In addition, we monitored changes in the cellular contents of parenchyma cells during the death of parenchyma cells.

Materials and methods

Plant materials and sample collection

In the present study, we used five *Cryptomeria japonica* trees. Sample collection date, age, tree height, diameter at breast height (DBH) and location information is shown in Table 1.

Block samples containing phloem, cambium and xylem were collected from the main stems at breast height during an active season of vascular cambium growth. To minimize the effect of wounding, samples were collected in different positions at the almost same height. Samples were fixed overnight at room temperature in a 5% (w/v) solution of glutaraldehyde in 0.1 M phosphate buffer (pH 7.2), and then the samples were washed with the same buffer.

Microscopy

Transverse and radial sections of approximately 40 µm thickness were cut on the freezing stage of a sliding microtome (Yamatokohki, Saitama, Japan).

Table 1 Sample collection dates, age, tree height, diameter at breast height (DBH) and location of sample trees

Sample tree	Sample collection dates	Age (years)	Tree height (m)	DBH (cm)	Location
A	2016/6/14, 7/14, 8/18	31	10	15.4	Field Museum Kusaki of TUAT[a]
B			11	15.9	
C	2017/6/6, 6/27, 7/12, 8/3, 2018/5/16	44	12	32.3	Fuchu campus of TUAT[b]
D		41	10	21.0	
E	2017/4/12, 5/15, 6/6, 6/27, 7/12, 8/3	14	9	21.0	

[a] Field Museum Kusaki of the Tokyo University of Agriculture and Technology (TUAT) in Midori-Gunma (36°32′ N, 139°25′ E), Japan

[b] The campus of the Tokyo University of Agriculture and Technology (TUAT) in Fuchu-Tokyo (35°68′ N, 139°48′ E), Japan

Unstained sections were mounted on glass slides in aqueous glycerol. To observe tissue and cell structure in secondary phloem and periderms, sections were examined under a light microscope (Axioscop.A1; Carl Zeiss, Oberkochen, Germany). After the light microscopic observations, the same sections were washed with distilled water and double-stained with fluorol yellow 088 (FY) and Congo red (CR) to detect suberized, lignified and non-lignified cell walls [26]. The FY was used for staining of suberized walls [27]. The CR was used for the staining of non–lignified walls [28]. Furthermore, lignified walls were detected using blue autofluorescence under ultra-violet excitation. Stained sections were observed under a confocal laser scanning microscope (LSM 710; Carl Zeiss; excitation/emission combination for detection of autofluorescence of lignin, 405 nm/BP 427–480; for detection of suberin stained with FY, 488 nm/BP 495–553 nm; and for detection of non-lignified walls stained with CR, 561 nm/BP 566–690 nm).

To record the emission spectra of the autofluorescence of cell walls of periderms, we examined sections in the "lambda scanning" mode with single-photon excitation under the confocal laser scanning microscope, which was equipped with a Plan Apochromat 20×/0.8 objective lens (Carl Zeiss), as described by Nakaba et al. [24]. Sequential single-plane images (1024 × 1024 pixels) were obtained at wavelengths from 417 to 727.4 nm and from 563 to 727.9 nm in steps of 9.7 nm with excitation at 405 nm and 561 nm, respectively. These obtained images were used to generate the lambda stack images with color using the ZEN 2010 software (Carl Zeiss). The relative intensity of autofluorescence as the brightness of captured digital images at each wavelength was recorded from ten randomly chosen pixels (0.415 × 0.415 μm^2) that distributed in the cell wall areas of periderms. Then, the average of values from the ten pixels was calculated.

In addition, radial sections were stained, separately with a 1% (w/v) aqueous solution of acetocarmine to observe nuclei [24, 29] or with a 1% (w/v) aqueous solution of iodine–potassium iodide (I_2–KI) to observe starch grains [24]. All sections were examined under a light microscope (Axioscop.A1; Carl Zeiss).

Results

We observed the process of rhytidome formation in five individual trees collected from 2016 to 2018. Although there were differences in the progress of rhytidome formation among sample trees and positions within each individual tree, all sample trees showed sequential changes in rhytidome formation from May to August. We classified the process of rhytidome formation into four stages based on the morphology as follows: just before the formation of new periderm (Stage 0); formation of new periderm (Stage 1); development of the new periderm (Stage 2); and maturation of new rhytidome (Stage 3).

Bark structure

Figure 1 shows the bark structure in transverse and radial plains in the stem of *Cryptomeria japonica*. The bark can be divided into two parts, namely inner bark and outer bark (rhytidome). The inner bark was observed as a pale-yellow area in unstained sections (Fig. 1a, b, e, f). In this area, it was easy to distinguish individual secondary phloem cells, such as sieve cells (S), phloem axial parenchyma cells (axial parenchyma cells, AP), phloem ray parenchyma cells (ray parenchyma cells, RP) and phloem fibers (F). These secondary phloem cells were arranged in a well-ordered manner. In contrast, the rhytidome was observed as a dark-brown area located outside the pale-yellow area in unstained sections (Fig. 1a, b, e, f). Under a confocal laser scanning microscope, the signals of FY were detected in one or two cell layers as shown by white arrows in Fig. 1. The cell layers stained with FY were considered to be phellem. Furthermore, the blue autofluorescence of phloem fibers with lignified walls was observed (Fig. 1c, d, g, h). In addition, several periderm layers that formed before the current year were observed in the rhytidome (Fig. 1c).

Stage 0: just before the formation of new periderm

In radial sections, the axial and ray parenchyma cells in the inner bark and the phelloderm of the innermost periderm contained nuclei that were stained with acetocarmine (black arrowheads in Fig. 2b). In addition, large amounts of starch grains stained with I_2–KI were observed in these parenchyma cells (white arrowheads in Fig. 2d). No clear difference in cell shape was observed in the phloem tissue around the innermost periderm that included no

(See figure on next page.)

Fig. 1 Conventional light and confocal laser scanning microscopic (CLSM) images showing the bark structure just before the formation of new periderm (Stage 0) in Tree A in June, 2016. Light micrographs of a transverse section (**a**, **e**) and a radial section (**b**, **f**) without staining showing the cell morphology and arrangement. **c**, **d**, **g**, **h** CLSM images of the same sections of **a**, **b**, **e**, **f** after stained with fluorol yellow 088 (FY) and Congo red (CR). **e**–**h** Higher magnification images of the selected areas in **a**–**d**. White arrows indicate the innermost periderms. AP axial parenchyma cell, F phloem fiber, IB inner bark, OB outer bark, Pd phelloderm, Pg phellogen, Ph phellem, Pr periderm, Rh rhytidome, RP ray parenchyma cell, S sieve cell. The right side of each micrograph corresponds to the outer side of the tree. Scale bars = 200 μm in **a**–**d**; 50 μm in **e**–**h**

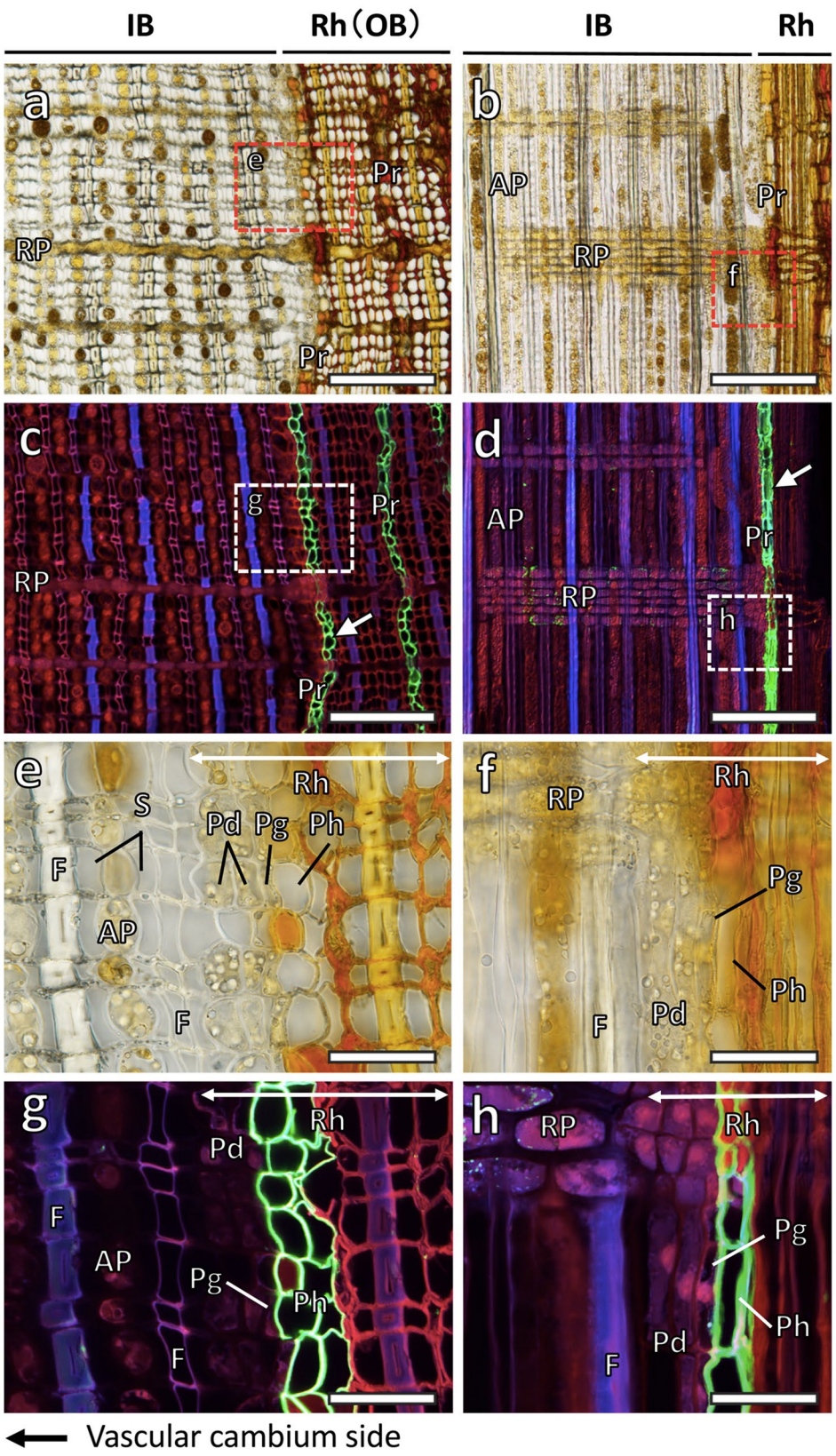

Fig. 1 (See legend on previous page.)

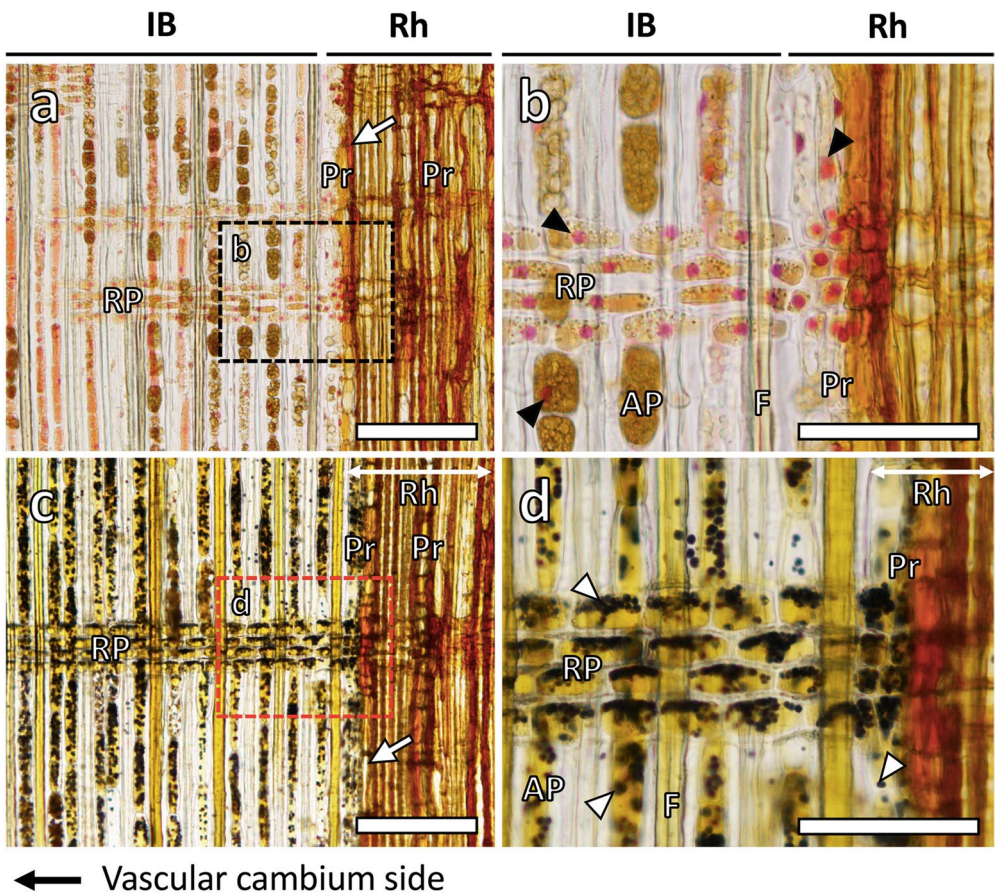

Fig. 2 Light micrographs of radial sections stained with acetocarmine (**a**, **b**) and iodine–potassium iodide (**c**, **d**), showing nuclei (black arrowheads) and starch grains (white arrowheads), just before the formation of new periderm (Stage 0) in Tree A in June, 2016. **b**, **d** Higher magnification images of the selected areas in **a**, **c**. White arrows indicate the innermost periderms. AP axial parenchyma cell, F phloem fiber, IB inner bark, Pr periderm, Rh rhytidome, RP ray parenchyma cell. The right side of each micrograph corresponds to the outer side of the tree. Scale bars = 200 µm in **a**, **c**; 100 µm in **b**, **d**

conducting phloem (Fig. 1a, b). In contrast, in the rhytidome, phloem and periderm cells contained no nuclei or starch grains and had brown cell walls (Figs. 1 and 2).

Stage 1: formation of new periderm

In transverse sections of the outer region of the inner bark, radially flattened cells were observed among the axial and ray parenchyma (white arrows in Fig. 3a, c). The meristematic appearance of such cells indicates that cell division occurred in axial and ray parenchyma leading to the formation of new periderm. The new periderm consisted of two to three cell layers in the radial direction. In these cells, no suberin signal by the FY staining in the cell walls was observed (Fig. 3b, d and Additional file 1: Fig. S1). Development of phellem and phelloderm was not yet distinguishable.

(See figure on next page.)

Fig. 3 Conventional light and CLSM images showing the formation of new periderm (Stage 1) in Tree B in June, 2016. **a**, **c** Light micrographs of a transverse section without staining. **b**, **d** CLSM images of the same section as in **a**, **c** after stained with FY and CR. Light micrographs of radial sections stained with acetocarmine (**e**, **f**) and iodine–potassium iodide (**g**), showing nuclei (black arrowheads) and starch grains, respectively. **c**, **d**, **f** Higher magnification images of the selected areas in **a**, **b**, **e**. Black arrows indicate axial and ray parenchyma cells with no nuclei. White arrows indicate new periderm. White arrowheads indicate new periderm with no starch grains. *AP* axial parenchyma cell, *F* phloem fiber, *IB* inner bark, *NPr* new periderm, *NRh* new prhytidome, *Pr* periderm, *Rh* rhytidome, *RP* ray parenchyma cell. The right side of each micrograph corresponds to the outer side of the tree. Scale bars = 200 µm in **a**, **b**, **e**; 100 µm in **f**, **g**; 50 µm in **c**, **d**

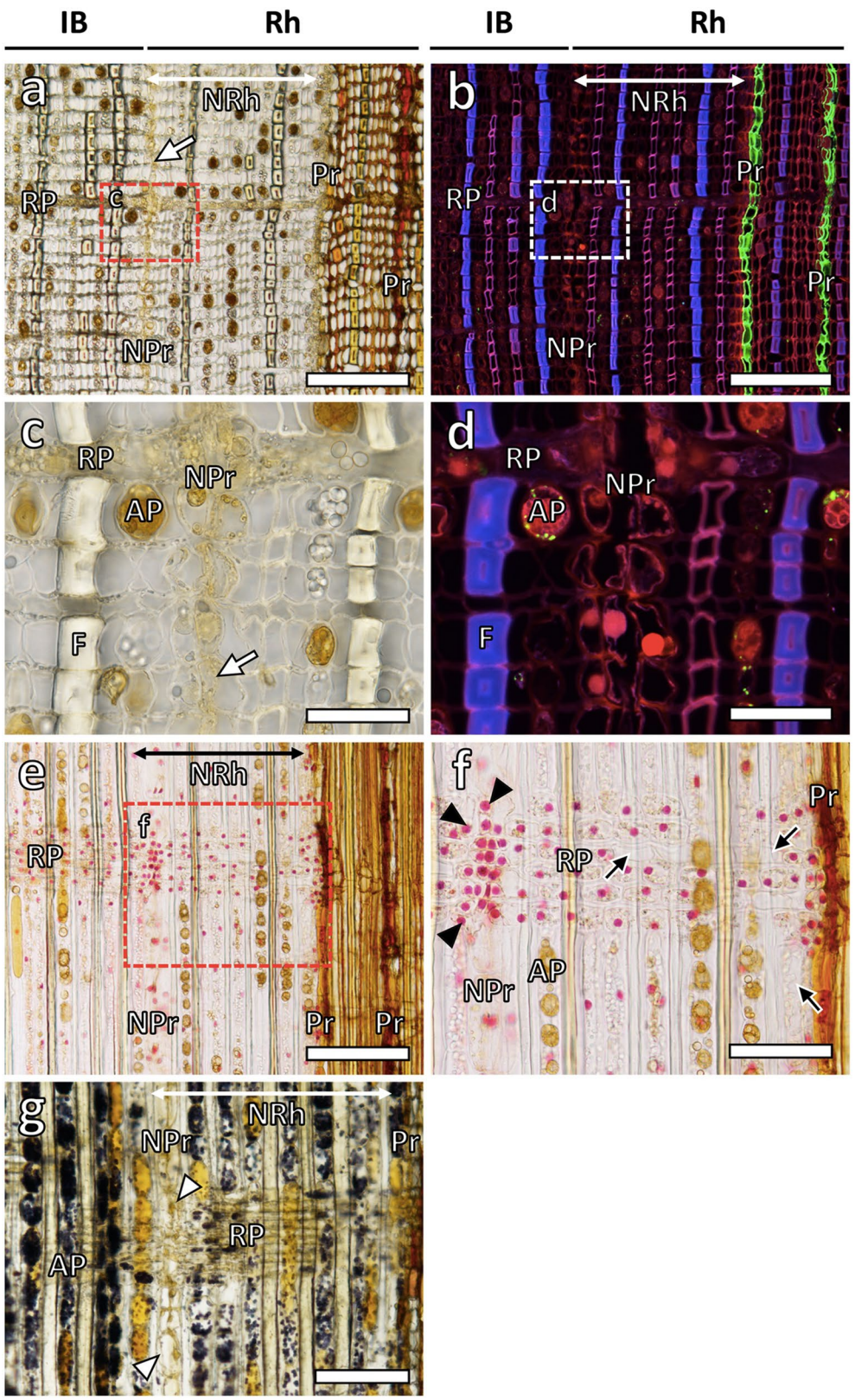

Fig. 3 (See legend on previous page.)

The cell walls of the phloem cells located outside the new periderm showed no dark-brown coloration as seen in the rhytidome. In radial sections, nuclei were distributed with high density in the new periderm in unstained sections (black arrowheads in Fig. 3f). In addition, sporadic disappearance of nuclei in axial and ray parenchyma was first observed in cell layers outside the new periderm (black arrows in Fig. 3f). In contrast, most of the phelloderm of the innermost periderm contained nuclei (Fig. 3f). Almost no starch grains were observed in the new periderm (white arrowheads in Fig. 3g). In addition, smaller amounts of starch grains were detected in axial and ray parenchyma cells outside the new periderm than in the cell layers on the inside of the new periderm (Fig. 3g).

Stage 2: development of the new periderm

An increased number of cells with the typical phellem cell shape could be seen in the new periderm (white arrows in Fig. 4c, d and Additional file 1: Fig. S2). Suberin signal by FY staining was detected in the thin cell walls of the outer 1–2 cell layers in this area (white arrows in Fig. 4b, d and Additional file 1: Fig. S2). Therefore, we identified these cell layers as new phellem that was produced by the new phellogen. On the other hand, FY signals from cell walls was not observed in the inner 1–2 cell layers (a yellow arrowhead in Fig. 4d). Therefore, these cells were distinguished as the phelloderm.

In the secondary phloem outside the new periderm, the cell walls were brighter colored compared with the cell walls of the rhytidome in unstained sections (Fig. 4a). In addition, the proportion of axial parenchyma cells without nuclei increased in the outer region of the new periderm in radial sections compared with Stage 1 (Fig. 4e, f). Decreased amounts of starch grains were observed across the entire inner bark and the new rhytidome, particularly in parenchyma cells outside the new periderm (white arrowheads in Fig. 4g, h). The phelloderm of the previous periderm had more nuclei and starch grains than the axial and ray parenchyma located between the new periderm and the previous periderm (Fig. 4e–h).

Stage 3: maturation of new rhytidome

The number of cells and the morphology of the new periderm in Stage 3 were similar to those of the new periderm in Stage 2. However, the phloem cells outside the new periderm had acquired brown cell walls that were strongly stained with FY (Fig. 5a–d and Additional file 1: Fig. S3). On the outer side of the new periderm, no cellular contents were observed in the axial parenchyma, making it indistinguishable from rhytidome (Fig. 5c, d). In radial sections, axial and ray parenchyma cells outside the new periderm had no nuclei or starch grains (Fig. 5e–h).

Figure 6 shows differences in the spectrum of autofluorescence between new and previous periderms in the transverse section in Stage 3. The emission spectrum under excitation at 561 nm of new periderm peaked at approximately 597 nm, while that of previous periderm peaked at approximately 636 nm (Fig. 6d). In addition, the relative intensity of fluorescence under excitation at 561 nm from previous periderm was higher than that from new periderm (Fig. 6d).

Figure 7 shows schematic diagrams describing the four stages of the new rhytidome formation. In addition, Table 2 shows the stages of rhytidome formation that were observed in each sample. There was no clear relationship between tree age and periderm formation among sample trees used in the present study. New rhytidome layers were formed during two consecutive years in trees C and D (Table 2).

Discussion

Timing of new rhytidome formation

In species that form rhytidome, the timing of sequent periderm formation varies depending on the tree species [2]. Mullick [30] pointed out that sequent periderms form at unpredictable intervals of time, making it inherently difficult to collect samples for developmental studies. This characteristic of sequent periderms has prevented

(See figure on next page.)

Fig. 4 Conventional light and CLSM images showing the development of a new periderm (Stage 2) in Tree A in August, 2016. **a**, **c** Light micrographs of a transverse section without staining. **b**, **d** CLSM images of the same section as in **a**, **c** after stained with FY and CR. Light micrographs of radial sections stained with acetocarmine (**e**, **f**) and iodine–potassium iodide (**g**, **h**), showing nuclei (black arrowheads) and starch grains, respectively. **c**, **d**, **f**, **h** Higher magnification images of the selected areas in **a**, **b**, **e**, **g**. Black arrows indicate axial and ray parenchyma cells with no nuclei. White arrows indicate the phellem cells of a new periderm. White arrowheads indicate axial and ray parenchyma cells outside the new periderm with no starch grains. Yellow arrows indicate phelloderm cells with starch grains in the previous periderm. Yellow arrowheads indicate phelloderm cells of new periderms. *AP* axial parenchyma cell, *F* phloem fiber, *IB* inner bark, *NPr* new periderm, *NRh* new rhytidome, *Pr* periderm, *Rh* rhytidome, *RP* ray parenchyma cell. The right side of each micrograph corresponds to the outer side of the tree. Scale bars = 200 µm in **a**, **b**; 100 µm in **e**, **f**, **g**, **h**; 50 µm in **c**, **d**

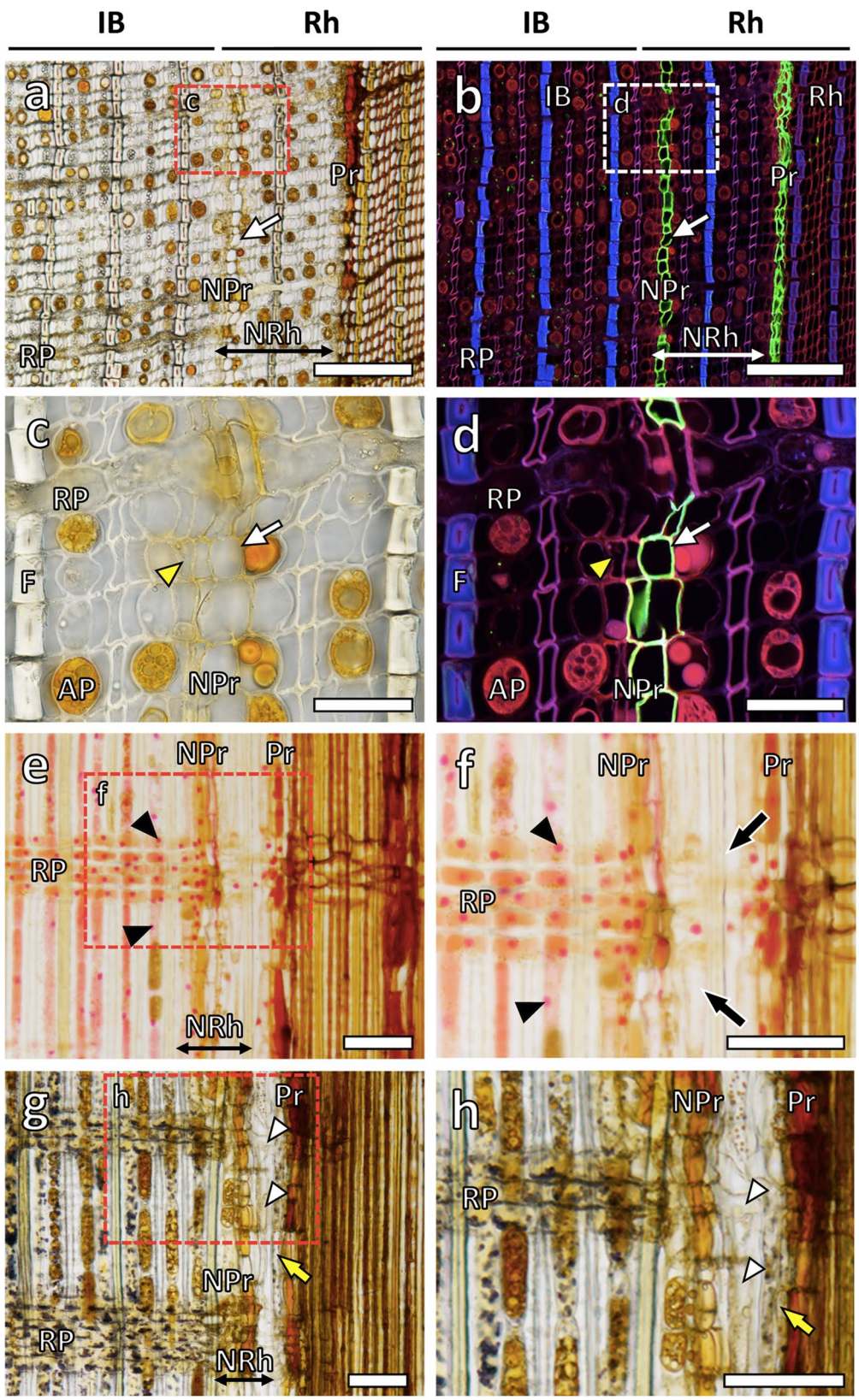

Fig. 4 (See legend on previous page.)

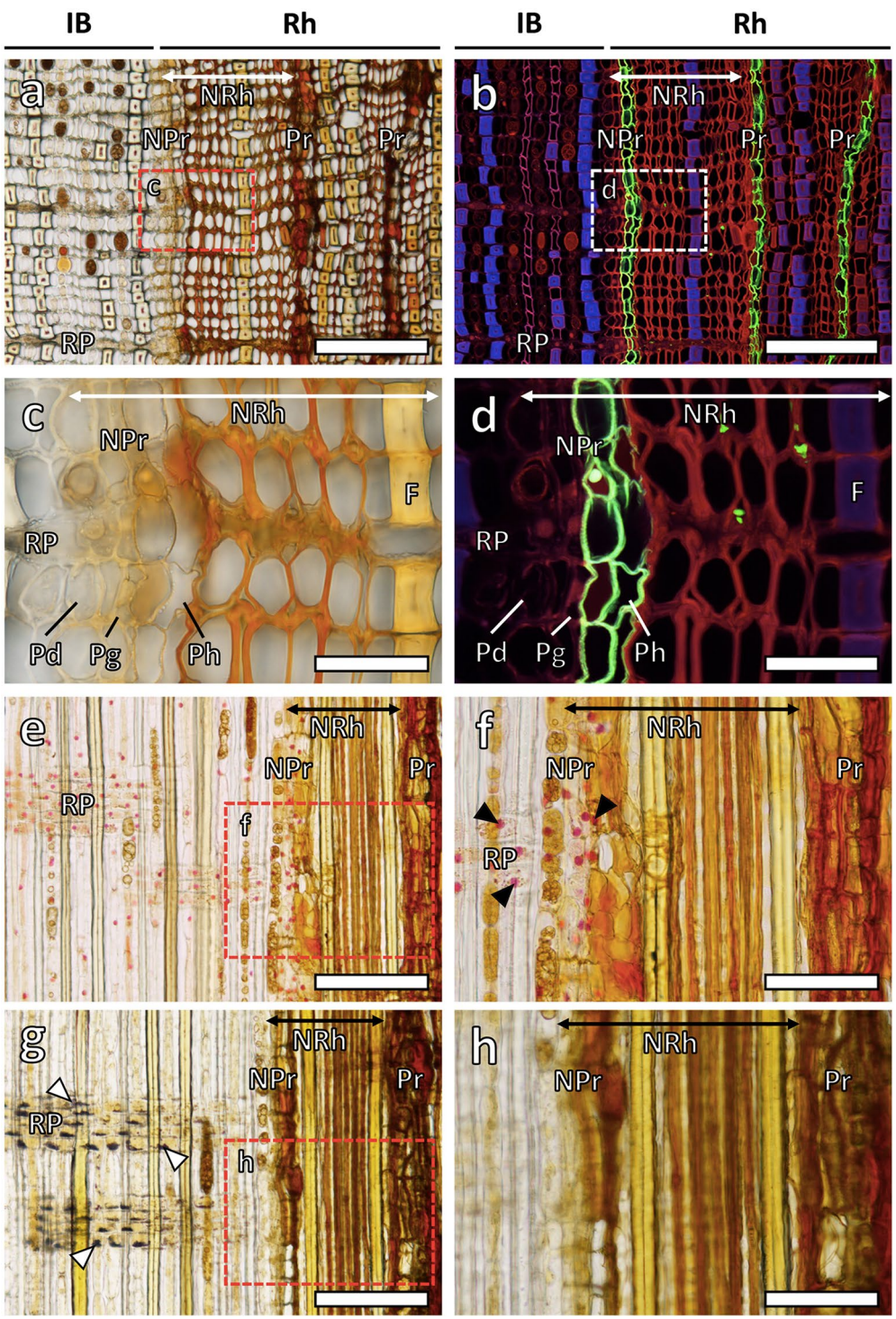

Fig. 5 Conventional light and CLSM images showing the maturation of new rhytidome (Stage 3) in Tree B in August, 2016. **a**, **c** Light micrographs of a transverse section without staining. **b**, **d** CLSM images of the same section as in **a**, **c** after stained with FY and CR. Light micrographs of radial sections stained with acetocarmine (**e**, **f**) and iodine–potassium iodide (**g**, **h**), showing nuclei and starch grains, respectively. **c**, **d**, **f**, **h** Higher magnification images of the selected areas in **a**, **b**, **e**, **g**. Black arrowheads indicate nuclei. White arrowheads indicate starch grains. *F* phloem fiber, *IB* inner bark, *NPr* new periderm, *NRh* new rhytidome, *Pd* phelloderm, *Pg* phellogen, *Ph* phellem, *Pr* periderm, *Rh* rhytidome, *RP* ray parenchyma cell. The right side of each micrograph corresponds to the outer side of the tree. Scale bars = 200 µm in **a**, **b**, **e**, **g**; 100 µm in **f**, **h;** 50 µm in **c**, **d**

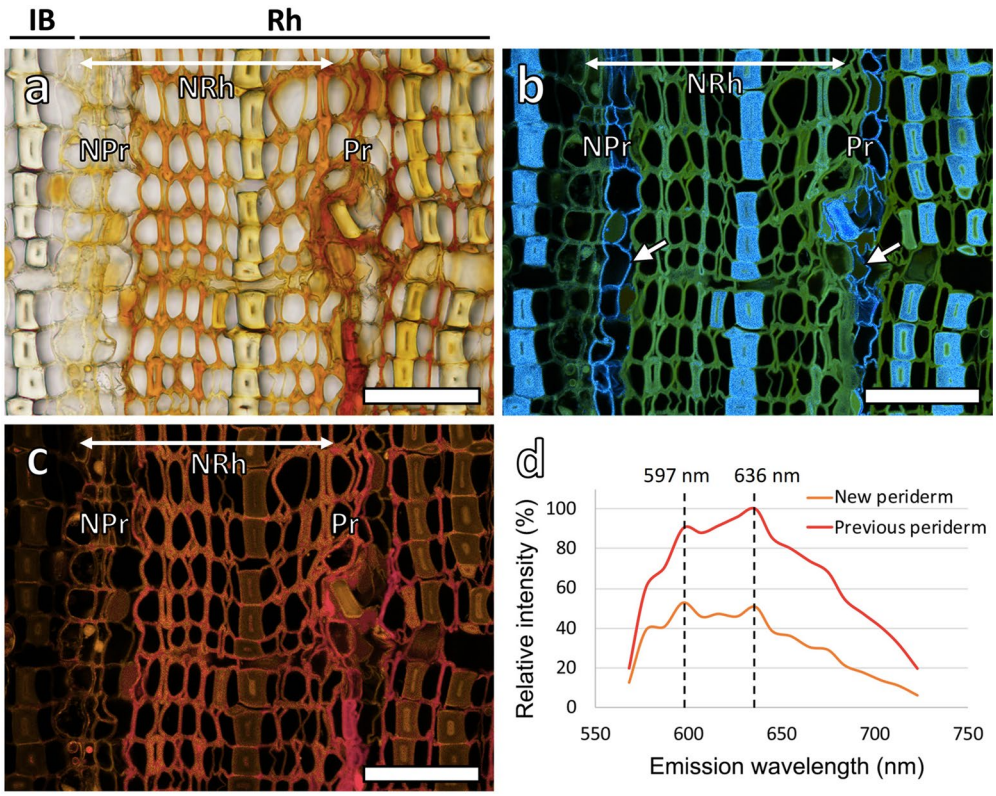

Fig. 6 Bright-field and autofluorescence images showing the new rhytidome at Stage 3 (**a**–**c**) in Tree B in August, 2016. **a** A light micrograph of a transverse section without staining. Lambda stack images of autofluorescence under fluorescence excitation at 405 nm (**b**) and 561 nm (**c**) obtained from the section in **a**. **d** Averaged emission spectra of autofluorescence under fluorescence excitation at 561 nm from ten randomly chosen pixels that distributed in the cell wall areas of new and previous periderms from the section in **a**–**c**. White arrows indicate phellem cells. *NPr* new periderm, *NRh* new rhytidome, *Rh* rhytidome. The right side of each micrograph corresponds to the outer side of the tree. Scale bars = 100 µm

the accumulation of definitive knowledge about their formation.

We detected new rhytidome formation in all individual trees of different ages and sizes (Table 2). In addition, new rhytidome formation was observed during two consecutive years in trees C and D (Table 2). These results indicate that new rhytidome formation occurs annually in *C. japonica*. Furthermore, new periderm formation and development were observed during May to July and June to August, respectively (Table 2). Our observations suggest that new periderm formation in *C. japonica* has seasonality. These characteristics of rhytidome formation indicate that we can follow the process of rhytidome formation in *C. japonica* by sequential sample collection in any given year. Therefore, we have confirmed that *C. japonica* is a suitable model species for analysis of the mechanism of periderm and rhytidome formation.

Process of new periderm and rhytidome formation

The process of rhytidome development in other conifer species was described by Mullick [6] using fluorescence microscopy with a cryofixation technique. In that study, the author focused on changes in pigment localization and the morphology and autofluorescence of cells. The present study enables us to discuss the timing of depletion of storage materials and cell death during new rhytidome formation.

The formation of new rhytidome proceeded in the order of Stages 0–3 as follows (Figs. 1, 2, 3, 4, 5, 7): start of cell division of axial and ray parenchyma cells in the outer region of the inner bark (formation of the new periderm),

Table 2 Stages of rhytidome formation in each sample

Sample tree	Sample collection dates (stage)
A	2016/6/14 (0, 1)[a], 7/14 (1), 8/18 (2)
B	2016/6/14 (1), 7/14 (2), 8/18 (3)
C	2017/6/6 (2), 6/27 (2), 7/12 (3), 8/3 (3), 2018/5/16 (1)
D	2017/6/6 (0), 6/27 (1), 7/12 (1), 8/3 (3), 2018/5/16 (1)
E	2017/4/12 (0), 5/15 (1), 6/6 (2), 6/27 (2), 7/12 (3), 8/3 (3)

[a] Stages 0 and 1 were observed in different parts of the same block sample

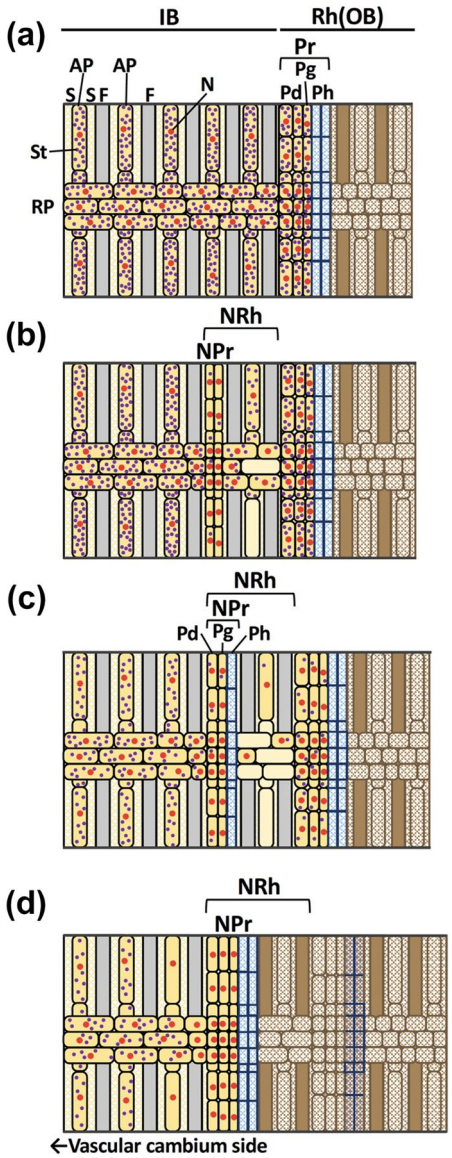

Fig. 7 Schematic diagrams showing the process of rhytidome formation in *Cryptomeria japonica* (in radial view). **a** Stage 0: all axial and ray parenchyma cells in the inner bark and innermost phelloderm contain nuclei and large amounts of starch grains. **b** Stage 1: a new periderm is formed from axial and ray parenchyma of the outer part of the inner bark. In the secondary phloem between the new periderm and previous periderm, sporadic disappearance of nuclei and decrease in the amounts of starch grains are observed in axial and ray parenchyma cells. **c** Stage 2: new phelloderm and phellem are producing, indicating the development of a new periderm. In the outer region of the new periderm, many axial parenchyma cells have no nuclei. The amount of starch grains decreases across the entire inner bark and new rhytidome, particularly in the parenchyma cells outside the new periderm. **d** Stage 3: the secondary phloem outside the new periderm become indistinguishable from the rhytidome with brown cell walls, no nuclei and no starch grains. *AP* axial parenchyma cell, *F* phloem fiber, *IB* inner bark, *N* nucleus, *NPr* new periderm, *NRh* new rhytidome, *Pr* periderm, *Pd* phelloderm, *Pg* phellogen, *Ph* phellem, *Rh (OB)* rhytidome (outer bark), *RP* ray parenchyma cell, *S* sieve cell, *St* starch grain

accompanied by a decrease in the amount of starch grains and sporadic disappearance of nuclei in axial and ray parenchyma cells outside the new periderm (Stage 1); formation of new phelloderm and phellem (development of new periderm; Stage 2); completion of cell death of phloem parenchyma cells sandwiched between the new periderm and the previous periderm, disappearance of starch grains and discoloration of the cell wall (Stage 3). We observed the same processes in all studied individual trees of different ages and sizes. At Stage 3, the peak of the emission spectrum, under excitation at 561 nm, from previous periderms occurred at a longer wavelength than that from new periderms (Fig. 6d). In addition, the intensity of autofluorescence, under excitation at 561 nm, from previous periderm was higher than that from new periderms (Fig. 6d). The peak shift from 597 to 636 nm and higher intensity of fluorescence indicate that some additional substances, which emitted autofluorescence with longer wavelength, have been accumulated in the cell walls of periderms. In *Quercus suber*, it has been reported that phenolic compounds accumulated in periderm and that genes involved in phenolic biosynthesis expressed in phellogen cells [19, 31]. Similarly, the biosynthesis of phenolic compounds might proceed in the phellogen cells in *Cryptomeria japonica*. Mullick [6] reported that dedifferentiating cells were significantly enlarged at the beginning of sequent periderm formation in young stems of *Tsuga heterophylla*. In transverse and radial sections, we detected no enlargement of parenchyma cells before new periderm formation at Stage 0 in the outer region of the inner bark of *C. japonica* (Figs. 1 and 2). The enlargement of cells prior to new periderm formation during sequent periderm formation might occur depending on the species and/or growth stage of the tree.

Sequent periderms have been classified as necrophylactic periderm that is formed on the inner side of necrotic tissue [5, 32]. Mullick [6] hypothesized that non-functionality of phellogen is the trigger for necrophylactic periderm formation and cell death itself is not the cause of rhytidome formation. However, the mechanism and function of the cell death that occurs outside the sequent periderm have not been discussed. In the present study, disappearance of nuclei was first observed in the phloem outside the newly formed periderm in radial sections of Stage 1 (Figs. 3 and 7). This observation indicates that

the parenchyma cells in the outer layers of the inner bark might have already been in a stage of preparation for cell death before the formation of the new periderm. Wunderling et al. [33] suggested that first periderm growth in the root and hypocotyl of *Arabidopsis thaliana* is tightly connected to the development of outside tissues and particularly to endodermal programmed cell death. Similarly, the death of parenchyma cells outside the new periderm might have an important role in periderm development.

When the periderm had developed with phelloderm and phellem (Stage 2), fewer starch grains were observed in the parenchyma cells outside the new periderm in radial sections (Figs. 4 and 7). Furthermore, after the formation of the new periderm was complete (Stage 3), the cellular contents of the parenchyma cells outside the new periderm disappeared, and the color of cell walls became brown and indistinguishable from the rhytidome that had been formed in the previous year (Figs. 5 and 7). O'Gara et al. [34] suggested that starch grains in the primary cortex adjacent to the region of periderm formation in *Eucalyptus marginata* seedlings might be used as a raw material for new cell production in the phellogen or as a precursor for phenolic compounds deposited in the periderm, including lignification of the thick-walled phellem. It is possible that starch in parenchyma cells outside the new periderm is used as an energy source and raw material for new cell production in the phellogen, or as a precursor for the biosynthesis of secondary metabolites such as suberin and phenolic compounds.

Conclusion

In the present study, we examined the histology of sequent periderm formation and the corresponding changes in the cellular contents of phloem parenchyma cells in *C. japonica*. We determined the following two characteristics of rhytidome formation: (1) periderm forms annually; therefore, it is possible to investigate the process of rhytidome formation in *C. japonica* by sequential sample collection in any given year; and (2) formation of new periderm and initiation of nuclei disappearance in phloem parenchyma outside the newly formed periderm appear to occur simultaneously. Four distinct stages of growth of the annual periderm and rhytidome were identified by histological observations. It is important to further investigate the changes of structure and vital state of the phloem parenchyma cells during rhytidome formation. Future studies should also add ultrastructural and molecular information to further elucidate the mechanism of rhytidome formation.

Supplementary Information

The online version contains supplementary material available at https://doi.org/10.1186/s10086-022-02027-4.

Additional file 1: Fig. S1. Conventional light and confocal laser scanning microscopic (CLSM) images showing the site of formation of new periderm (Stage 1) in Tree B in June, 2016. (**a**) A light micrograph of a radial section without staining. (**b**) A CLSM image of the same section of (**a**) after stained with fluorol yellow 088 (FY) and Congo red (CR). IB inner bark, NPr new periderm, NRh new rhytidome, Pr periderm, Rh rhytidome, RP ray parenchyma cell. The right side of each micrograph corresponds to the outer side of the tree. Scale bars = 200 µm. **Fig. S2.** Conventional light and CLSM images showing the development of a new periderm (Stage 2) in Tree A in August, 2016. (**a**, **c**) Light micrographs of a radial section without staining. (**b**, **d**) CLSM images of the same sections as in (**a**, **c**) after stained with FY and CR. (**c**, **d**) Higher magnification images of the selected areas in (**a**, **b**). White arrows indicate the phellem cells of a new periderm. AP axial parenchyma cell, F phloem fiber, IB inner bark, NPr new periderm, NRh new rhytidome, Pr periderm, Rh rhytidome, RP ray parenchyma cell. The right side of each micrograph corresponds to the outer side of the tree. Scale bars = 200 µm in **a**, **b**; 50 µm in **c**, **d**. **Fig. S3.** Conventional light and CLSM images showing the maturation of new rhytidome (Stage 3) in Tree B in August, 2016. (**a**, **c**) Light micrographs of a radial section without staining. (**b**, **d**) CLSM images of the same sections as in (**a**, **c**) after stained with FY and CR. (**c**, **d**) Higher magnification images of the selected areas in (**a**, **b**). F phloem fiber, IB inner bark, NPr new periderm, NRh new rhytidome, Pr periderm, Rh rhytidome, RP ray parenchyma cell. The right side of each micrograph corresponds to the outer side of the tree. Scale bars = 200 µm in **a**, **b**; 50 µm in **c**, **d**

Acknowledgements

The authors thank the staff of the Field Museum Kusaki of the Tokyo University of Agriculture and Technology for providing plant materials. The authors also thank Mr. Eisaku Iyoshi and Ms. Ayumi Kurita (Faculty of Agriculture, Tokyo University of Agriculture and Technology) for support the experiments.

Authors' contributions

MO, RI, EI, IA, PK, RF and SN conceived and designed the experiment. MO, RI, EI performed the experiments and data analysis. MO wrote the manuscript. All authors read and approved the final manuscript.

Funding

This work was supported by JSPS KAKENHI Grant Numbers JP18H02251, JP18H02258, JP19H03014 and JP20K21327.

Availability of data and materials

Not applicable.

Declarations

Competing interests

The authors declare that they have no competing interests.

Author details

[1]Faculty of Agriculture, Tokyo University of Agriculture and Technology, 3-5-8 Saiwai-cho, Fuchu, Tokyo 183-8509, Japan. [2]Institute of Global Innovation Research, Tokyo University of Agriculture and Technology, Fuchu, Tokyo 183-8538, Japan. [3]School of Environmental and Forest Sciences, University of Washington, Seattle, WA 98195, USA.

Received: 24 November 2021 Accepted: 13 March 2022
Published online: 27 March 2022

References

1. Trockenbrodt M (1990) Survey and discussion of the terminology used in bark anatomy. IAWA Bull 11:141–166. https://doi.org/10.1163/22941932-90000511
2. Evert RF (2006) Esau's plant anatomy: meristems, cells, and tissues of the plant body—their structure, function, and development, 3rd edn. Wiley, New Jersey
3. Angyalossy V, Pace MR, Evert RF, Marcati CR, Oskolski AA, Terrazas T, Kotina E, Lens F, Mazzoni-Viveiros SC, Angeles G, Machado SR, Crivellaro A, Rao KS, Leo J, Nikolaeva N, Baas P (2016) IAWA list of microscopic bark features. IAWA J 37:517–615. https://doi.org/10.1163/22941932-20160151
4. Srivastava LM (1964) Anatomy, chemistry, and physiology of bark. In: Romberger JA, Mikola P (eds) International review of forestry research, vol 1. Academic Press Inc., New York, pp 203–277
5. Mullick DB, Jensen GD (1973) New concepts and terminology of coniferous periderms: necrophylactic and exophylactic periderms. Can J Bot 51:1459–1470. https://doi.org/10.1139/b73-185
6. Mullick DB (1977) The non-specific nature of defense in bark and wood during wounding, insect and pathogen attack. In: Loewus FA, Runeckles VC (eds) The structure, biosynthesis, and degradation of wood. Springer, Boston, pp 395–441
7. Borger GA, Kozlowski TT (1972) Effects of light intensity on early periderm and xylem development in *Pinus resinosa*, *Fraxinus pennsylvanica*, and *Robinia pseudoacacia*. Can J For Res 2:190–197. https://doi.org/10.1139/x72-033
8. Lev-Yadun S, Aloni R (1990) Polar patterns of periderm ontogeny, their relationship to leaves and buds, and the control of cork formation. IAWA Bull 11:289–300. https://doi.org/10.1163/22941932-90001185
9. Arzee T, Liphschitz N, Waisel Y (1968) The origin and development of the phellogen in *Robinia pseudacadia* L. New Phytol 67:87–93. https://doi.org/10.1111/j.1469-8137.1968.tb05457.x
10. Borger GA, Kozlowski TT (1972) Effects of photoperiod on early periderm and xylem development in *Fraxinus Pennsylvanica*, *Robinia pseudoacacia* and *Ailanthus altissima* seedlings. New Phytol 71:703–708. https://doi.org/10.1111/j.1469-8137.1972.tb01281.x
11. Borger GA, Kozlowski TT (1972) Effects of temperature on first periderm and xylem development in *Fraxinus pennsylvanica*, *Robinia pseudoacacia*, and *Ailanthus altissima*. Can J For Res 2:198–205. https://doi.org/10.1139/x72-034
12. Borger GA, Kozlowski TT (1972) Effects of cotyledons, leaves and stem apex on early periderm development in *Fraxinus pennsylvanica* seedlings. New Phytol 71:691–702. https://doi.org/10.1111/j.1469-8137.1972.tb01280.x
13. Pereira H (2007) Cork biology production and uses. Elsevier, Amsterdam
14. Graça J, Pereira H (2004) The periderm development in *Quercus suber*. IAWA J 25:325–335. https://doi.org/10.1163/22941932-90000369
15. Gričar J, Jagodic Š, Prislan P (2015) Structure and subsequent seasonal changes in the bark of sessile oak (*Quercus petraea*). Trees 29:747–757. https://doi.org/10.1007/s00468-015-1153-z
16. Miguel A, Milhinhos A, Novák O, Jones B, Miguel CM (2016) The *SHORT-ROOT*-like gene *PtSHR2B* is involved in *Populus* phellogen activity. J Exp Bot 67:1545–1555. https://doi.org/10.1093/jxb/erv547
17. Rains MK, Gardiyehewa de Silva ND, Molina I (2018) Reconstructing the suberin pathway in poplar by chemical and transcriptomic analysis of bark tissues. Tree Physiol 38:340–361. https://doi.org/10.1093/treephys/tpx060
18. Shibui H, Sano Y (2018) Structure and formation of phellem of *Betula maximowicziana*. IAWA J 39:18–36. https://doi.org/10.1163/22941932-20170186
19. Teixeira RT, Fortes AM, Bai H, Pinheiro C, Pereira H (2018) Transcriptional profiling of cork oak phellogenic cells isolated by laser microdissection. Planta 247:317–338. https://doi.org/10.1007/s00425-017-2786-5
20. Alonso-Serra J, Safronov O, Lim KJ, Fraser-Miller SJ, Blokhina OB, Campilho A, Chong SL, Fagerstedt K, Haavikko R, Helariutta Y, Immanen J, Kangasjärvi J, Kauppila TJ, Lehtonen M, Ragni L, Rajaraman S, Räsänen RM, Safdari P, Tenkanen M, Yli-Kauhaluoma JT, Teeri TH, Strachan CJ, Nieminen K, Salojärvi J (2019) Tissue-specific study across the stem reveals the chemistry and transcriptome dynamics of birch bark. New Phytol 222:1816–1831. https://doi.org/10.1111/nph.15725
21. Shigematsu Y (1960) Studies on the structure of bark. V. On the arrangements of bark elements of Sugi (*Cryptomeria japonica* D. Don.). Rep Kyoto Pref Univ Agr 12:106–112 (**In Japanese with English summary**)
22. Kitin P, Fujii T, Abe H, Takata K (2009) Anatomical features that facilitate radial flow across growth rings and from xylem to cambium in *Cryptomeria japonica*. Ann Bot 103:1145–1157. https://doi.org/10.1093/aob/mcp050
23. Nakaba S, Arakawa I, Morimoto H, Nakada R, Bito N, Imai T, Funada R (2016) Agatharesinol biosynthesis-related changes of ray parenchyma in sapwood sticks of *Cryptomeria japonica* during cell death. Planta 243:1225–1236. https://doi.org/10.1007/s00425-016-2473-y
24. Nakaba S, Morimoto H, Arakawa I, Yamagishi Y, Nakada R, Funada R (2017) Responses of ray parenchyma cells to wounding differ between earlywood and latewood in the sapwood of *Cryptomeria japonica*. Trees 31:27–39. https://doi.org/10.1007/s00468-016-1452-z
25. Kuroda K, Yamane K, Ito Y (2020) Radial movement of minerals in the trunks of standing Japanese cedar (*Cryptomeria japonica* D. Don) trees in summer by tracer analysis. Forests 11:562. https://doi.org/10.3390/f11050562
26. Kitin P, Nakaba S, Hunt CG, Lim S, Funada R (2020) Direct fluorescence imaging of lignocellulosic and suberized cell walls in roots and stems. AoB PLANTS 12:plaa032. https://doi.org/10.1093/aobpla/plaa032
27. Brundrett MC, Kendrick B, Peterson CA (1991) Efficient lipid staining in plant material with sudan red 7B or fluorol yellow 088 in polyethylene glycol-glycerol. Biotech Histochem 67:111–116. https://doi.org/10.3109/10520299109110562
28. Nakaba S, Kitin P, Yamagishi Y, Begum S, Kudo K, Nugroho WD, Funada R (2015) Three-dimensional imaging of cambium and secondary xylem cells by confocal laser scanning microscopy. In: Yeung ECT, Stasolla C, Sumner MJ, Huang BQ (eds) Plant microtechniques and protocols. Springer, Berlin, pp 431–465. https://doi.org/10.1007/978-3-319-19944-3_24
29. Arakawa I, Funada R, Nakaba S (2018) Changes in the morphology and functions of vacuoles during the death of ray parenchyma cells in *Cryptomeria japonica*. J Wood Sci 64:177–185. https://doi.org/10.1007/s10086-017-1692-6
30. Mullick DB (1971) Natural pigment differences distinguish first and sequent periderms of conifers through a cryofixation and chemical techniques. Can J Bot 49:1703–1711. https://doi.org/10.1139/b71-240
31. Teixeira RT, Fortes AM, Pinheiro C, Pereira H (2014) Comparison of good- and bad-quality cork: application of high-throughput sequencing of phellogenic tissue. J Exp Bot 65:4887–4905. https://doi.org/10.1093/jxb/eru252
32. Mullick DB (1975) A new tissue essential to necrophylactic periderm formation in the bark of four conifers. Can J Bot 53:2443–2457. https://doi.org/10.1139/b75-271
33. Wunderling A, Ripper D, Barra-Jimenez A, Mahn S, Sajak K, Targem MB, Ragni L (2018) A molecular framework to study periderm formation in *Arabidopsis*. New Phytol 219:216–229. https://doi.org/10.1111/nph.15128
34. O'Gara E, Howard K, Colquhoun IJ, Dell B, McComb J, Hardy GESJ (2009) The development and characteristics of periderm and rhytidome in *Eucalyptus marginata*. Aust J Bot 57:221–228. https://doi.org/10.1071/BT08225

Publisher's Note